JOC The Journal of Organic Chemistry

Article

pubs.acs.org/joc

Tuning of Excited-State Intramolecular Proton Transfer (ESIPT) Fluorescence of Imidazo[1,2-*a*]pyridine in Rigid Matrices by Substitution Effect

Toshiki Mutai,* Hirotaka Sawatani, Toshihide Shida, Hideaki Shono, and Koji Araki*

Department of Materials and Environmental Science, Institute of Industrial Science, The University of Tokyo, 4-6-1, Komaba, Meguro-ku, Tokyo 153-8505, Japan

Supporting Information

ABSTRACT: 2-(2′-Hydroxyphenyl)imidazo[1,2-*a*]pyridine (HPIP, **1**) and its derivatives are synthesized, and their fluorescence properties are studied. Although all the compounds show faint dual emission ($\Phi \approx 0.01$), which is assigned to the normal and excited-state intramolecular proton transfer (ESIPT) fluorescence in a fluid solution, they generally display efficient ESIPT fluorescence (Φ up to 0.6) in a polymer matrix. The introduction of electron-donating and electron-withdrawing groups into the phenyl ring causes blue and red shifts of the ESIPT fluorescence emission band, respectively. On the other hand, the introduction of such groups into the imidazopyridine part results in fluorescence shifts in the opposite directions. The results of ab initio quantum chemical calculations of the intramolecular proton-transferred (IPT) state are well in line with the ESIPT fluorescence energies. The plots of the calculated highest occupied molecular orbital (HOMO) and lowest unoccupied molecular orbital (LUMO) energy levels against the Hammett substituent constants (σ) show good linearity with different slopes, which can rationalize the effect of the substituent and its position on the IPT state. Therefore, we have developed a series of HPIPs as new ESIPT fluorescent compounds and demonstrate that ESIPT fluorescence properties would be rationally tuned using quantum chemical methods.

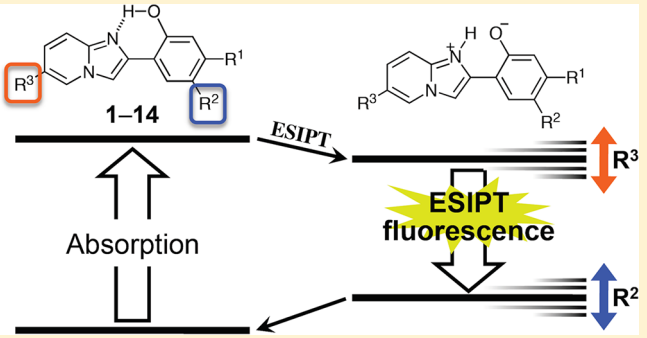

INTRODUCTION

Organic solid-state luminescent materials have been attracting considerable attention because they have various applications.[1] Whereas solid-state luminescent materials are generally designed from the compounds that exhibit efficient fluorescence in solution, it is well-known that luminescence is quenched in the solid state as a result of intermolecular interactions, which enhance nonradiative deactivation of the excited state.

In recent years, there has been growing interest in organic compounds that are nonemissive in the solution state but efficiently luminescent in a rigid environment.[2] In general, such compounds have two or more aromatic groups connected by a single bond. Enhanced emission is caused by restricting the intramolecular rotation around the single bond. These compounds would be good candidates for new solid-state luminophores, since they have not been considered as light emitters.

A photoinduced proton transfer through an intramolecular hydrogen bond is termed excited-state intramolecular proton transfer (ESIPT),[3] which is a remarkably fast process (rate constant $k \approx 1 \times 10^{13}$ s^{-1}; Scheme 1a).[4] Emission from the ESIPT state[5] is characterized by a large Stokes shift ($\approx 10\,000$ cm^{-1}), which enables long-wavelength fluorescence by UV excitation, but the fluorescence quantum yield is generally low. To date, the most studied compounds, because of their efficient ESIPT fluorescence, are 2-(2′-hydroxyphenyl)benzimidazole (HBI),[6] 2-(2′-hydroxyphenyl)benzoxazole (HBO),[7] 2-(2′-hydroxyphenyl)benzothiazole (HBT)[8] (Scheme 1b), and their analogues.

Luminescent behavior in the solid state is a major current topic,[9] and there have been some reports of solid-state ESIPT luminescence[6a,8a,10,11] and basic application to electroluminescent devices[8a,12,13] and white luminescent materials.[13,14] However, the development of such systems remains a challenge because compounds exhibiting efficient solid-state ESIPT luminescence have been limited to date. In addition, it is generally difficult to tune known fluorophores to give desirable photophysical properties by chemical modification, because a small structural alteration often impairs their fluorescence properties.

We have previously reported[11] that 2-(2′-hydroxyphenyl)-imidazo[1,2-*a*]pyridine (HPIP, **1**, Scheme 1c) exhibits efficient ESIPT luminescence in the solid state, and we also found that **1** forms two crystal polymorphs that exhibit bright ESIPT luminescences of different colors, namely, blue-green (496 nm, $\Phi = 0.50$) and yellow (529 nm, $\Phi = 0.37$). However, there

Received: December 13, 2012

   dx.doi.org/10.1021/jo302711t | J. Org. Chem. XXXX, XXX, XXX–XXX

Scheme 1[a]

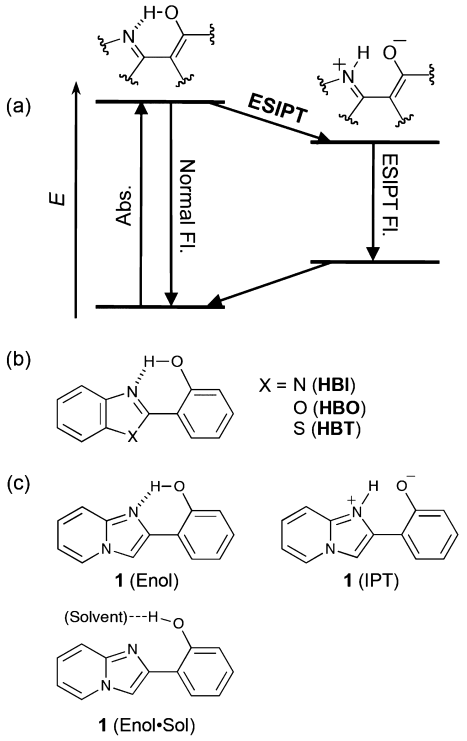

[a](a) The energy diagram of ESIPT process. (b) Molecular structure of well-studied benzazoles exhibiting ESIPT fluorescence. (c) The enol, IPT, and solvated enol (Enol·Sol) forms of 2-(2′-hydroxyphenyl)-imidazo[1,2-*a*]pyridine (HPIP, **1**).

has been no systematic study of the luminescent properties of HPIP derivatives because of their very low emission quantum yields in organic fluid solutions ($\Phi \approx 0.01$).[15−17] Our recent quantum chemical study[18] on the potential energy surfaces in the ground (S_0) and excited (S_1) states showed that the ESIPT state (S_1) smoothly approached the S_0−S_1 conical intersection, coupled with twisting motion around the central C−C single bond connecting the phenyl and imidazo[1,2-*a*]pyridine rings. The S_0−S_1 energy gap was sufficiently small at the dihedral angle of 60° for rapid radiationless decay in a fluid solution. Therefore, the remarkable emission enhancement for solid HPIP was assigned to suppression of the efficient radiationless decay by fixing the dihedral angle at a nearly coplanar orientation in a rigid environment.

In this study, we synthesized various HPIP derivatives and studied their ESIPT fluorescence properties. Though all the HPIPs showed quite weak fluorescence in fluid organic solutions, they displayed efficient fluorescence in rigid media ($\Phi \approx 0.6$). A wide range of solid-state ESIPT fluorescence was achieved with good quantum efficiency. Furthermore, the ESIPT fluorescence of HPIPs was simulated by molecular orbital calculations, and the results were well in line with the experimental data. The ESIPT fluorescence could be rationally controlled by shifting the energy level of either the lowest unoccupied molecular orbital (LUMO) or the highest occupied molecular orbital (HOMO) of the intramolecular proton-transferred (IPT) state.

RESULTS AND DISCUSSION

Synthesis. A series of HPIPs were synthesized through reaction of 2-aminopyridine and α-bromoacetophenone, forming the imidazo[1,2-*a*]pyridine core (Scheme 2). Starting from reactants with various R^1, R^2, and R^3, the reaction yielded

Scheme 2. Synthetic Scheme of 1−14[a]

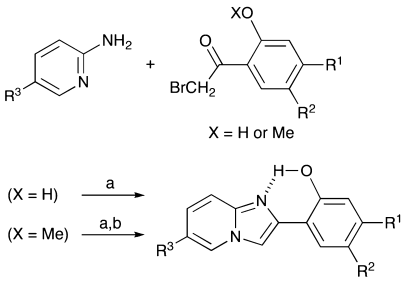

	R^1	R^2	R^3		R^1	R^2	R^3
1	H	H	H	**8**	H	H	Cl
2	H	OMe	H	**9**	H	H	Br
3	H	Me	H	**10**	H	H	CF_3
4	H	Cl	H	**11**	H	H	CN
5	H	Br	H	**12**	OMe	H	H
6	H	F	H	**13**	H	Me	Cl
7	H	H	Me	**14**	H	Me	CF_3

[a](a) $NaHCO_3$, CH_3CN, reflux, 20 h; (b) BBr_3, CH_2Cl_2, 15 h.

compounds **2**−**14**. 5′-Substituted HPIPs **2**−**6** were synthesized by coupling of 2-aminopyridine and 4-substituted 2-(bromoacetyl)phenol (R^2 = OMe, Me, Cl, Br, F). 6-Substituted HPIPs (**7**−**11**) were obtained by reaction of 5-substituted 2-aminopyridine (R^3 = Me, Cl, Br, F, CF_3, CN) and 2-(bromoacetyl)anisole. The resultant methoxy intermediates were demethylated by tribromoborane. 4′-Methoxy-**12** and 5′,6-disubstituted HPIPs **13** and **14** were synthesized similarly to 5′-substituted HPIPs. All compounds were obtained as colorless microcrystalline powders.

Absorption Properties in Fluid and Rigid Media. As representative examples of phenyl- and imidazopyridyl-substituted HPIPs, the absorption and fluorescence spectra of 5′-bromo (**5**) and 6-bromo (**9**) HPIP in tetrahydrofuran (THF) are presented in Figure 1. In a fluid THF solution, π−π^* absorption bands of both compounds appeared at around 340 nm. As shown in Table 1, the absorption spectra of 5′-substituted (**2**−**6**), 6-substituted (**7**−**11**), 4′-substituted (**12**),

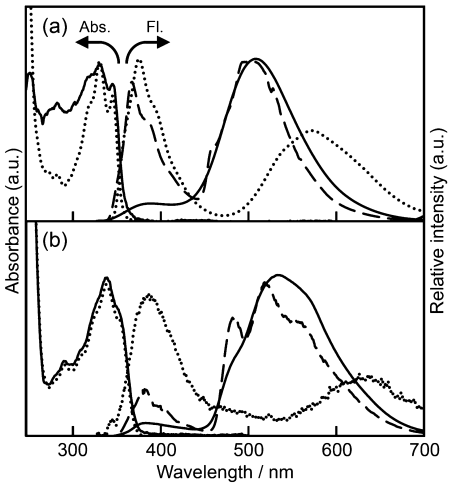

Figure 1. Absorption and emission spectra of **5** (a) and **9** (b) in a THF solution at room temperature (dotted line), at 77 K (broken line), and in a PMMA film (solid line).

dx.doi.org/10.1021/jo302711t | J. Org. Chem. XXXX, XXX, XXX−XXX

Table 1. Absorption and Fluorescence Maxima of 1−14

	THF (rt)		THF (77 K)	PMMA	
	λ_{abs}/nm	λ_{em}/nm	λ_{em}/nm	λ_{abs}/nm	λ_{em}/nm (Φ)
1	333 (1.02)	377, 602 (0.08)	370, 521	331	520 (0.37)
2	352.5 (1.36), 339 (1.47)	384 (0.01)	376, 571	336	381, 565 (0.06)
3	334 (1.38)	382, 620 (0.01)	370, 535	332	530 (0.31)
4	333.5 (1.39)	378, 576 (0.02)	369, 513	333	509 (0.42)
5	333.5 (1.47), 348 (1.15)	378, 573 (0.01)	370, 507	333, 348	510 (0.57)
6	333.5 (1.11)	379, 597 (0.02)	370, 531	332	514 (0.37)
7	331 (1.12)	381, 588 (0.02)	368, 518	331	378, 522 (0.35)
8	340 (1.05)	392, 634 (<0.01)	383, 549	340	539 (0.23)
9	341 (1.08)	390, 640 (<0.01)	383, 523	340	533 (0.16)
10	339 (1.08)	398 (0.01)	392, 543	331	390, 541 (0.20)
11	336.5 (1.01)	399, 569 (0.01)	401, 545	351	399, 561 (0.13)
12	333.5 (1.44)	386, 577 (0.01)	378, 529	336	514 (0.61)
13	343 (1.52)	395 (0.01)	388, 571	343	389, 571 (0.09)
14	342 (1.18)	401 (<0.01)	396	342	390, 570 (0.06)

and disubstituted (**13**, **14**) HPIPs appeared in the near-UV region in fluid THF solution, with a maximum wavelength in the range 333−341 nm. Such marginal differences in the absorption spectra indicate that substitution has little effect on the absorption properties of HPIP **1**.

The absorption properties of **1**−**14** in the solid state were then examined by preparing a transparent poly(methyl methacrylate) (PMMA) film containing 0.5 wt % of each HPIP derivative by the spin-coating method. The transmission absorption spectra of **1**−**14** were quite similar in terms of shape and maximum wavelength, comparable to those observed in dilute THF solution, indicating that the HPIPs existed as monomers in the PMMA matrix and were insusceptible to a rigid environment (Figure 1, Table 1).

Fluorescence Properties in Fluid and Rigid Media. On excitation at 330 nm, compounds **5** and **9** exhibited weak dual emission (Φ ≈ 0.01) at 378 and 573 nm for **5** and at 390 and 640 nm for **9** in dilute THF solution. The excitation spectra of the two emission bands of **5** and **9** were similar to the corresponding absorption spectra, indicating that both emissions originated from single molecule species. By comparing the dual emission bands with the reported fluorescence spectra of the parent compound **1**,[15] the near-UV emission was assigned to a normal fluorescence from the enol species that is not intramolecularly hydrogen-bonded due to solvation (**1** Enol·Sol, Scheme 1c), and that with a large Stokes shift (ca. 12 000 cm^{-1}) is the ESIPT fluorescence (Scheme 1a). Although the normal fluorescence emissions of **1**, **5**, and **9** appeared in a similar region, the ESIPT fluorescence emissions differed significantly. Whereas a blue shift (ca. 30 nm/840 cm^{-1}) of the ESIPT fluorescence was observed for the 5′-bromo derivative, an opposite red shift with a similar value (ca. 40 nm/990 cm^{-1}) was observed for the 6-bromo derivative **9**, suggesting that the ESIPT fluorescence would be tunable not only by substituent, but also by substituting position.

In a frozen THF solution at 77 K, the emission intensified more than 50-fold. The ESIPT fluorescence bands of **5** and **9** shifted to significantly shorter wavelengths, 507 and 549 nm, respectively, whereas the excitation spectrum appeared in the same region as for a fluid solution. In contrast, the normal fluorescence (ca. 380 nm) did not show a notable shift.

The emission upon excitation at 330 nm was similarly intense and blue-shifted in a PMMA matrix. It is worth noting that ESIPT fluorescence was the only or dominant emission in PMMA. The quantum yields of **5** and **9** rose to 0.57 and 0.16, respectively, which is an order of magnitude larger than those in a fluid THF solution.

Previously, we studied the polymorph-dependent ESIPT luminescence of **1** and concluded that the blue-green (496 nm, Φ = 0.50) and yellow (529 nm, Φ = 0.37) luminescence could be assigned to the coplanar and twisted species, respectively.[11] Therefore, the yellow ESIPT fluorescence emissions of **1** in a frozen THF solution (521 nm) and PMMA matrix (520 nm) indicate that **1** might form a planar conformation in these rigid media.

As shown in Table 1, the ESIPT fluorescence was very weak for all HPIPs in a fluid THF solution (Φ ≈ 0.01), but was quite efficient in a PMMA matrix (Φ = 0.1−0.6). A blue shift (50−90 nm/2 100−3 600 cm^{-1}) of the ESIPT fluorescence was observed for all HPIPs, regardless of the substituent and its position, suggesting that the blue shift could be attributed to the effect of the rigid environment. The fluorescence decays of **1**−**14** in a PMMA matrix fitted reasonably with a biexponential curve (τ_1 = 0.8−1.6 ns, τ_2 = 2.9−5.4 ns; χ^2 = 0.9−1.2). The weighted average lifetimes (τ_M) of all the compounds were 2.1−4.9 ns, indicating singlet emission.

It was reported by Douhal et al.[15,16] that a zwitterionic ESIPT species further transitioned to the twisted conformation (Figure 2) along with rearrangement of surrounding solvent molecules in a fluid solution, which could be the reason for the significantly large Stokes shift. Our recent study on the potential energy surfaces in the ground (S_0) and excited (S_1) states of **1** supports this discussion;[18] the S_0−S_1 gap energy (i.e., the ESIPT fluorescence energy) decreases with increasing the dihedral angle (θ) between phenyl and imidazo[1,2-

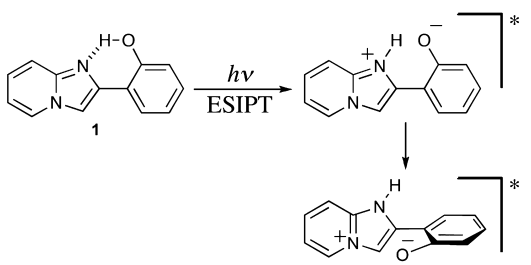

Figure 2. The proton transfer and subsequent twisting motion of HPIP (**1**) in the excited state.

dx.doi.org/10.1021/jo302711t | J. Org. Chem. XXXX, XXX, XXX−XXX

a]pyridine rings. Because such molecular motion processes are suppressed in the rigid environments, the ESIPT species retains the planar conformation and thereby emits the blue-shifted ESIPT fluorescence. A similar environmental effect has been found for twisted intramolecular charge-transfer (TICT) emission,[19] which has been reported[20] to show a blue shift in rigid media.

A gradual red shift of the ESIPT fluorescence was observed when the electron-donating nature of the 5′-substituent increased. On the other hand, the ESIPT fluorescence showed a blue shift on introducing an electron-donating group at the 6 position, indicating the opposite substituent effect. In the case of disubstituted HPIPs **13** and **14**, the ESIPT fluorescence emissions were observed at much longer wavelengths compared with the corresponding monosubstituted HPIPs **3**, **8**, and **10**. The lower-energy fluorescence might be the result of the cumulative effect of two substitutions.

Chemical alteration of a fluorophore often causes undesirable perturbation to its emissive electronic state and results in impairment of its fluorescence properties. However, in the case of HPIPs, substitution of either the phenyl or imidazo[1,2-*a*]pyridine ring schematically altered the color of the ESIPT fluorescence in the solid matrix, while retaining reasonable quantum efficiency. Because substituted HPIPs are readily available using various commercially available aminopyridines and hydroxyacetophenones, substitution of HPIP is a simple and useful method for tuning color without damaging the luminescent nature in the solid state.

Theoretical Simulation of Substituent Effect. To understand the effect of substituents further, the electronic states of HPIPs were studied using ab initio quantum chemical calculations. Geometry optimization of the enol form of **1** by an RHF/6-31G(d) calculation resulted in a coplanar conformation as the energy-minimum structure, which was further applied to a single-point energy calculation including the diffuse function (RHF/6-31+G(d)). The lowest-energy absorption band was shown to be the HOMO−LUMO transition. Both the HOMO and LUMO of the enol form were delocalized over a molecule (Figure 3). The same calculation was also applied to **2**−**14**, and it was found that the electronic configurations of the aromatic core of HOMO and LUMO were qualitatively similar to that of **1**.

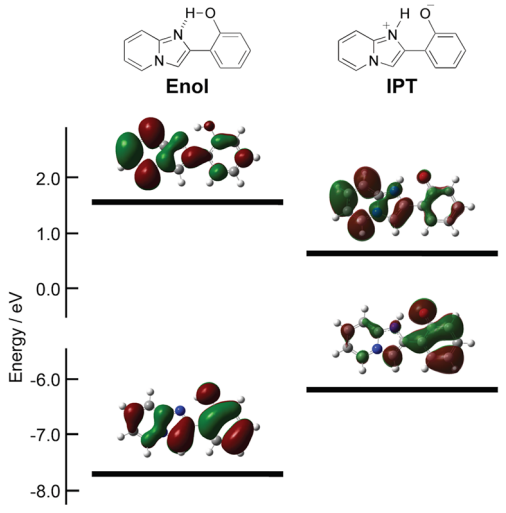

Figure 3. Molecular orbitals of the enol and IPT forms of **1** that participate in the ESIPT process.

Then the excited electronic state of the IPT form was calculated using the CI-Single method (CIS/6-31+G(d)) after geometry optimization by CIS/6-31G(d). The lowest-energy transition band, which corresponds to the ESIPT fluorescence, was calculated to be HOMO−LUMO. Unlike the enol form, the HOMO and LUMO of the IPT form, $HOMO_{IPT}$ and $LUMO_{IPT}$, were localized mainly on the imidazo[1,2-*a*]pyridine and phenyl ring, respectively (Figure 3).

The measured ESIPT emission energies of **1**−**14** in a PMMA matrix were plotted against the calculated energies of the $HOMO_{IPT}$−$LUMO_{IPT}$ transitions (Figure 4). Although the estimated values of the transition energy were somewhat larger (ca. 0.9 eV) than the observed energies (Table S1, Supporting Information), the linear correlation of the plots (R^2 = 0.91) confirmed that the quantum chemical simulation was effective for qualitative reproduction of the observed ESIPT fluorescence emissions of HPIPs.

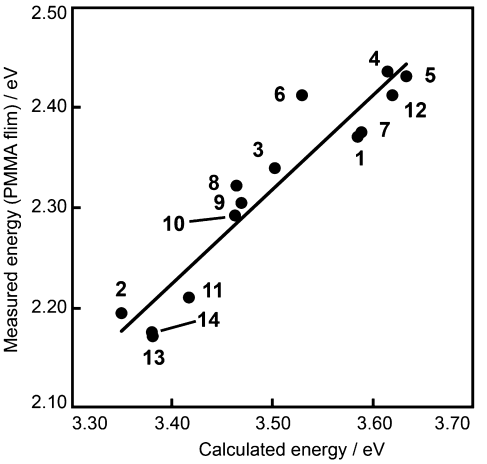

Figure 4. Plot of the calculated against measured energy of ESIPT fluorescence of **1**−**14**.

It has been reported that the Hammett substituent constant (σ) could be a useful parameter for explaining the substituent effect on the emission properties.[21] Thus, the calculated energy levels of $HOMO_{IPT}$ and $LUMO_{IPT}$ (Table S1, Supporting Information) of 5′-substituted and 6-substituted HPIPs were plotted against Hammett substituent constants, as shown in Figure 5.

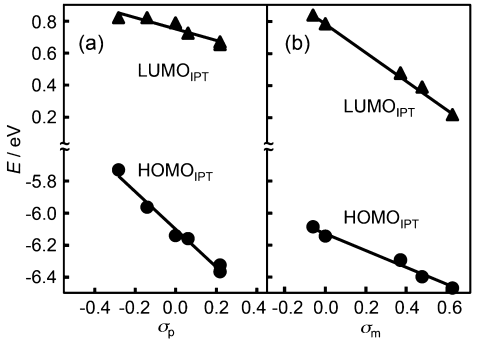

Figure 5. Plot of the calculated energy levels of $HOMO_{IPT}$ and $LUMO_{IPT}$ against the Hammett substituent constants (σ_p or σ_m). (a) 5′-Substituted HPIP (**2**−**6**), and (b) 6-substituted HPIP (**7**−**11**).

dx.doi.org/10.1021/jo302711t | J. Org. Chem. XXXX, XXX, XXX−XXX

As shown in Figure 5a, the energy levels of 5′-substituted HPIPs are well correlated with the Hammett *para*-substituent constant (σ_p; R^2 = 0.98 for $HOMO_{IPT}$, 0.88 for $LUMO_{IPT}$), but not against the Hammett *meta*-substituent constant (σ_m; R^2 = 0.46 for $HOMO_{IPT}$, 0.83 for $LUMO_{IPT}$). The energy gap became larger when the value of σ_p increased, which is consistent with the observed blue shift of the ESIPT fluorescence. More importantly, the energy level of $HOMO_{IPT}$ decreased more steeply than that of $LUMO_{IPT}$, indicating that substitution at the 5′ position had a larger electronic effect on $HOMO_{IPT}$. This could be ascribed to the localized electron density on the phenyl ring in $HOMO_{IPT}$ compared with $LUMO_{IPT}$, which was supported by the ab initio calculation (Figure 3).

In the case of 6-substituted HPIPs (Figure 5b), the energy levels were linearly fitted against σ_m (R^2 = 0.98 for $HOMO_{IPT}$, 0.99 for $LUMO_{IPT}$) instead of σ_p (R^2 = 0.90 for $HOMO_{IPT}$, 0.80 for $LUMO_{IPT}$). The smaller energy gap with increasing σ_m value is consistent with the observed red shift of the ESIPT fluorescence. Opposite to 5′-substituted HPIPs, the energy level of $LUMO_{IPT}$ decreased more steeply than that of $HOMO_{IPT}$ when the value of σ_m increased. The larger effect of 6-substitution on the energy level of $LUMO_{IPT}$ was assigned to the larger electron density on the imidazo[1,2-*a*]pyridine ring in $LUMO_{IPT}$, as was shown by the quantum chemical calculations (Figure 3).

It is noteworthy that the energy levels of $HOMO_{IPT}$ and $LUMO_{IPT}$ 5′,6-disubstituted HPIPs could be estimated by summation of the substituent effect on each aromatic ring. In a comparison of 5′-methyl-6-chloro-HPIP **13** and **1**, the energy level of $HOMO_{IPT}$ was higher (−6.11 eV for **13** and −6.14 eV for **1**), whereas that of $LUMO_{IPT}$ was lower (0.51 eV for **13** and 0.79 eV for **1**; Table S1, Supporting Information). This result indicates dominant effects of 5′-methyl and 6-chloro substituents with respect to the energy levels of $HOMO_{IPT}$ and $LUMO_{IPT}$, respectively, which is in good agreement with the above-discussed effect of monosubstitution and with the observed lower-energy fluorescence emissions of the disubstituted HPIPs. The same result was obtained by a comparison of 5′-methyl-6-(trifluoromethyl)-HPIP **14** and **1**.

Thus, the substituent effects on the ESIPT fluorescence emissions of monosubstituted HPIPs were reasonably explained by the ab initio quantum chemical calculations. A noteworthy correlation between the energy levels and Hammett substituent constants (σ_m, σ_p) indicates that the orbital energies were principally determined by the electronic properties of those substituents.

The key to such schematically controllable properties of the ESIPT fluorescence emissions of HPIPs is $HOMO_{IPT}$ and $LUMO_{IPT}$, in which the electrons are localized on the phenyl ring and imidazo[1,2-*a*]pyridine ring, respectively.

CONCLUSION

The synthesis of 2-(2′-hydroxyphenyl)imidazo[1,2-*a*]pyridine (HPIP, **1**) and its derivatives (**2**−**14**) was described, and substituent effects on the ESIPT fluorescence properties were studied. Although all compounds showed faint dual emission ($\Phi \approx 0.01$), ascribed to normal and ESIPT fluorescences in a fluid solution, they generally displayed bright ESIPT fluorescence in a polymer matrix (Φ = 0.1−0.6). The introduction of electron-donating and electron-withdrawing groups into the phenyl ring (**2**−**6**) caused blue and red shifts of the ESIPT fluorescence, respectively. On the other hand, introduction of these groups into the imidazopyridine part (**7**−**11**) resulted in fluorescence shifts in the opposite direction. The plots of the calculated $HOMO_{IPT}$ and $LUMO_{IPT}$ energy levels against the Hammett substituent constants (σ) showed good linearities with different slopes, which rationally explain the effect of the substituent and its position on the IPT state. Thus, a series of HPIPs as new ESIPT fluorescent compounds were developed, and substituent effects on the ESIPT fluorescence properties were successfully reproduced and explained by the electronic configurations and energy levels of $HOMO_{IPT}$ and $LUMO_{IPT}$. It is suggested that ESIPT fluorescence properties might be predictable using quantum chemical simulations.

EXPERIMENTAL SECTION

Methods. ^{1}H NMR peaks were assigned using H−H COSY and heteronuclear multiple quantum coherence (HMQC) methods. UV−vis absorption and fluorescence spectra in organic solutions were recorded using standard spectrophotometer and spectrofluorophotometer, respectively. The fluorescence quantum yield in a fluid THF solution was calculated using 2-aminopyridine (Φ = 0.37; ethanol; excitation wavelength 285 nm) as a standard. Time-resolved emission decay was recorded by exciting samples with a nitrogen laser pulse (337 nm).

The fluorescence spectra in a PMMA matrix were measured in an integral sphere attatched to a spectrofluorophotometer, and the quantum yield was obtained using calculation software based on the literature method,[22] which was installed in the spectrofluorophotometer.

The energy levels of HOMO and LUMO of the enol form were calculated by the HF method after geometry optimization (HF/6-31G+(d)//HF/6-31G(d)), and those of $HOMO_{IPT}$ and $LUMO_{IPT}$, corresponding to ESIPT and IPT states, were calculated by the CI-Single method (CIS/6-31+G(d)//CIS/6-31G(d)). These calculations were performed using a Gaussian 03W, Gaussian Inc. (Revision C.02) package,[23] and the results were processed on a GaussView 4.1 or a Fujitsu Scigress Explorer (Version 7).

Materials. 2-Bromo-1-(2-methoxyphenyl)ethanone was purchased from Wako Chemical Co. 3-Bromo-, 5-bromo-, and 3,5-dibromo-2-aminopyridines, and other chemicals, were also commercially available and used as received. The syntheses of 2-(2′-hydroxyphenyl)imidazo-[1,2-*a*]pyridine (**1**) and 2-(2′-methoxyphenyl)imidazo[1,2-*a*]pyridine (**10**) have been described elsewhere.[11]

Transparent polymer films were prepared from a benzene solution of PMMA (200 mg in 2 mL) containing 0.5 wt % of each HPIP derivative by spin-coating method (500 μL, 1000 rpm, 15 s.).

General Synthetic Procedure for 5′-Substituted 2-(2′-Hydroxyphenyl)imidazo[1,2-*a*]pyridine (5′-Substituted HPIP). A chloroform solution of corresponding 4-substituted 2-acetylphenol and copper(II) bromide (1.5 equiv) was refluxed for 16 h. After cooling, filtering off insoluble solid, evaporation of the filtrate yielded crude 4-substituted 2-(bromoacetyl)phenol, which was applied to a silica gel column ($CHCl_3$). Then an acetonitrile solution of 4-substituted 2-(bromoacetyl)phenol, 2-aminopyridine, and $NaHCO_3$ (2 equiv) was refluxed for 18 h. After filtering off insoluble solid and evaporation, the crude product was purified by a silica gel column chromatography (eluent for each compound shown below).

*5′-Methoxy HPIP (**2**).* Eluent: $CHCl_3$/hexane = 1:2. Further recrystallization from ethanol afforded white crystal (235 mg, 69%): mp 126.4−126.9 °C; ^{1}H NMR ($CDCl_3$, 400 MHz) δ 12.26 (1H, s, OH), 8.16 (1H, dd, J = 5.5, 1.1 Hz, 5-H), 7.86 (1H, s, 3-H), 7.60 (1H, d, J = 8.2 Hz, 8-H), 7.22−7.26 (1H, m, 7-H), 7.12 (1H, d, J = 2.7 Hz, 6-H), 6.98 (1H, d, J = 8.8 Hz, 3′-H), 6.83−6.88 (2H, m, 4′,6-H), 3.82 (3H, s, OCH_3); ^{13}C NMR ($CDCl_3$, 100 MHz) δ 152.2, 151.5, 145.1, 143.5, 125.4, 125.2, 118.17, 116.8, 116.2, 115.7, 113.1, 110.5, 106.8, 55.9. Anal. Calcd for $C_{14}H_{12}N_2O_2$: C,69.99; H,5.03; N,11.66%. Found: C,69.64; H,5.02; N,11.39%.

dx.doi.org/10.1021/jo302711t | J. Org. Chem. XXXX, XXX, XXX−XXX

*5′-Methyl HPIP (**3**).* Eluent: $CHCl_3$/hexane = 5:1. Further recrystallization from ethanol afforded white crystal (413 mg, 39%): mp 150.9−151.2 °C; ^{1}H NMR ($CDCl_3$, 400 MHz) δ 12.48 (1H, s, OH), 8.14 (1H, d, J = 6.6 Hz, 5-H), 7.85 (1H, s, 3-H), 7.57 (1H, t, J = 4.9 Hz, 8-H), 7.39 (1H, d, J = 1.6 Hz, 6′-H), 7.22 (1H, ddd, J = 9.1, 6.9, 1.4 Hz, 7-H), 7.04 (1H, dd, J = 8.2, 1.6 Hz, 4′-H), 6.94 (1H, d, J = 8.2 Hz, 3′-H), 6.84 (1H, td, J = 7.0, 1.2 Hz, 6-H), 2.32 (3H, s, CH_3); ^{13}C NMR ($CDCl_3$, 100 MHz) δ 155.1, 145.4, 143.4, 130.4, 127.9, 125.9, 125.3, 125.0, 117.4, 116.7, 115.7, 113.1, 106.6, 20.6. Anal. Calcd for $C_{14}H_{12}N_2O$: C,74.98; H,5.39; N,12.49%. Found: C,75.02; H,5.35; N,12.34%.

*5′-Chloro HPIP (**4**).* Eluent: $CHCl_3$/hexane = 2:1. Further recrystallization from ethanol afforded white crystal (616 mg, 61%): mp 188.0−188.8 °C; ^{1}H NMR ($CDCl_3$, 400 MHz) δ 12.74 (1H, s, OH), 8.17 (1H, d, J = 7.1 Hz, 5-H), 7.87 (1H, s, 3-H), 7.61 (1H, d, J = 9.3 Hz, 8-H), 7.55 (1H, d, J = 2.7 Hz, 6′-H), 7.25−7.32 (1H, m, 7-H), 7.17 (1H, dd, J = 8.5, 2.5 Hz, 4′-H), 6.97 (1H, d, J = 8.8 Hz, 3′-H), 6.89 (1H, td, J = 6.8, 1.2 Hz, 6-H); ^{13}C NMR ($CDCl_3$, 100 MHz) δ 155.9, 144.1, 143.5, 129.3, 126.6, 125.5, 125.2, 123.5, 119.1, 117.4, 116.9, 113.4, 107.0. Anal. Calcd for $C_{13}H_9ClN_2O$: C,63.81; H,3.71; N,11.45%. Found: C,63.54; H,3.69; N,11.23%.

*5′-Bromo HPIP (**5**).* Eluent: $CHCl_3$/hexane = 1:1. Further recrystallization from ethanol afforded white crystal (1.78 g, 60%): mp 198.6−199.5 °C; ^{1}H NMR ($CDCl_3$, 400 MHz) δ 12.77 (1H, s, OH), 8.17 (1H, d, J = 7.1 Hz, 5-H), 7.86 (1H, s, 3-H), 7.69 (1H, d, J = 2.2 Hz6′-H), 7.60 (1H, d, J = 9.3 Hz, 8-H), 7.25−7.31 (2H, m, 4′,7-H), 6.90 (2H, dd, J = 14.8, 7.7 Hz, 3′,6-H); ^{13}C NMR ($CDCl_3$, 100 MHz) δ 156.4, 143.9, 143.4, 132.1, 128.1, 125.6, 125.5, 119.5, 118.0, 116.8, 113.4, 110.6, 107.0. Anal. Calcd for $C_{13}H_9BrN_2O$: C,54.00; H,3.14; N,9.69%. Found: C,53.90; H,3.11; N,9.39%.

*5′-Fluoro HPIP (**6**).* Eluent: $CHCl_3$. Further recrystallization from ethanol afforded white crystal (346 mg, 44%): mp 161.6−162.6 °C; ^{1}H NMR ($CDCl_3$, 400 MHz) δ 12.51 (1H, s, OH), 8.18 (1H, d, J = 6.9 Hz, 5-H), 7.85 (1H, s, 3-H), 7.61 (1H, d, J = 9.2 Hz, 8-H), 7.25−7.29 (2H, m, 6′,7-H), 6.93−6.99 (2H, m, 3′,4′-H), 6.89 (1H, t, J = 6.9 Hz, 6-H); ^{13}C NMR ($CDCl_3$, 100 MHz) δ 157.0, 154.7, 153.4, 144.4, 143.5, 125.5, 118.5, 116.9, 116.4, 116.2, 113.4, 111.5, 111.3, 107.1. Anal. Calcd for $C_{13}H_9FN_2O$: C,68.42; H,3.97; N,12.27%. Found: C,68.16; H,3.94; N,12.16%.

General Synthetic Procedure for 6-Substituted 2-(2′-Hydroxyphenyl)imidazo[1,2-*a*]pyridine (6-Substituted HPIP). An acetonitrile solution of 2-(bromoacetyl)anisol, 5-substituted 2-amino-pyridine and $NaHCO_3$ (2 equiv) was refluxed for 20 h. After filtering off insoluble solid, the filtrate was evaporated, and the residue was applied to a silica gel column ($CHCl_3$/ethyl acetate =10:1) to afforded 6-substituted 2-(2′-methoxyphenyl) imidazo[1,2-*a*]pyridine. A dichloromethane solution of boron tribromide (1.0 M, 4 equiv) was dropwise added to a cooled anhydrous dichloromethane solution of well-dried 6-substituted 2-(2′-methoxyphenyl) imidazo[1,2-*a*]pyridine. The reaction mixture was allowed to reach room temperature and further stirred for 15 h. A saturated aqueous $NaHCO_3$ was slowly added with stirring, and then was separated with water and chloroform. After washing the organic layer with saturated aqueous $NaHCO_3$ and water, and drying over Na_2SO_4, the organic layer was evaporated to give crude product.

*HPIP (**1**).* Purification by recrystallization from ethanol (3.65 g, 43%): mp 142−143 °C; ^{1}H NMR ($CDCl_3$, 400 MHz) δ 12.70 (1H, s, OH), 8.16 (1H, dd, J = 5.5, 1.1 Hz, 5-H), 7.88 (1H, s, 3-H), 7.60 (2H, dd, J = 8.0, 1.4 Hz, 6′,8-H), 7.21−7.25 (2H, m, 4′,7-H), 7.04 (1H, dd, J = 8.2, 1.1 Hz, 3′-H), 6.85−6.91 (2H, m, 5′,6-H); ^{13}C NMR ($CDCl_3$, 100 MHz) δ 157.3, 145.3, 143.4, 129.7, 125.7, 125.4, 125.2, 119.0, 117.7, 116.8, 116.2, 113.2, 106.7. Anal. Calcd for $C_{13}H_{10}N_2O$: C,74.27; H,4.79; N,13.33%. Found: C,74.02; H,4.81; N,13.30%.

*6-Methyl HPIP (**7**).* Purification by recrystallization from ethanol (820 mg, 38%): mp 180.6−181.5 °C; ^{1}H NMR ($CDCl_3$, 400 MHz) δ 7.92(1H, s, 5-H), 7.77(1H, s, 3-H), 7.57(1H, dd, J = 6.0, 1.0 Hz, 6′-H), 7.49(1H, d, J = 9.2 Hz, 8-H), 7.21(1H, td, J = 5.4, 1.0 Hz, 4′-H), 7.02−09(2H, m, 3′,7-H), 6.87(1H, td, J = 4.8, 0.8 Hz, 5′-H), 2.34(s, 3H, CH_3); ^{13}C NMR ($CDCl_3$, 100 MHz) δ 157.3, 145.0, 142.4, 129.4, 128.3, 125.6, 123.1, 122.8, 118.9, 117.6, 116.4, 116.1, 106.4, 18.2. Anal. Calcd for $C_{14}H_{12}N_2O$: C,74.98; H,5.39; N,12.49. Found: C,75.19; H,5.26; N,12.42.

*6-Chloro HPIP (**8**).* Purification by a silica gel column chromatography ($CHCl_3$) and recrystallization from dimethyl sulfoxide yielded **8** as white solid (1.26 g, 76%): mp 197.6−198.5 °C; ^{1}H NMR ($CDCl_3$, 400 MHz) δ 12.41 (1H, s, OH), 8.19 (1H, dd, J = 1.8, 0.9 Hz, 5-H), 7.83 (1H, d, J = 0.7 Hz, 3-H), 7.58−7.52 (2H, m, 6′,8-H), 7.23−7.27 (1H, m, 4′-H), 7.20 (1H, dd, J = 9.5, 1.9 Hz, 7-H), 7.04 (1H, dd, J = 8.2, 1.1 Hz, 3′-H), 6.89 (1H, ddd, J = 8.1, 6.8, 0.9 Hz, 5′-H); ^{13}C NMR ($CDCl_3$, 100 MHz) δ 157.2, 146.3, 141.9, 130.0, 126.5, 125.8, 123.2, 121.3, 119.1, 117.8, 117.0, 115.7, 107.1. Anal. Calcd for $C_{13}H_9ClN_2O$: C,63.81; H,3.71; N,11.45%. Found: C,63.70; H,3.67; N,11.31%.

*6-Bromo HPIP (**9**).* Purification by a silica gel column chromatography ($CHCl_3$) afforded **9** as white powder (166 mg, 72%): mp 207.5−208.6 °C; ^{1}H NMR ($CDCl_3$, 400 MHz) δ 12.39 (1H, s, OH), 8.30 (1H, d, J = 1.1 Hz, 5-H), 7.83 (1H, s, 3-H), 7.57 (1H, dd, J = 7.7, 1.6 Hz, 6′-H), 7.49 (1H, t, J = 7.7 Hz, 8-H), 7.23−7.31 (2H, m, 4′,7-H), 7.04 (1H, dd, J = 8.2, 1.1 Hz, 3′-H), 6.89 (1H, td, J = 7.4, 1.2 Hz, 5′-H); ^{13}C NMR ($CDCl_3$, 100 MHz) δ 157.3, 146.2, 141.9, 130.0, 128.6, 125.8, 125.3, 119.1, 117.8, 117.3, 115.7, 107.7, 106.9. Anal. Calcd for $C_{13}H_9BrN_2O$: C,54.00; H,3.14; N,9.69%. Found: C,53.82; H,3.07; N,9.43%.

*6-Trifluoromethyl HPIP (**10**).* Purification by a silica gel column chromatography ($CHCl_3$) yielded **10** as white powder (423 mg, 44%): mp 229.9−231.0 °C; ^{1}H NMR ($CDCl_3$, 400 MHz) δ 12.27(1H, s, OH), 8.55(1H, s, 5-H), 7.97(1H, s, 3-H), 7.71(1H, d, J = 7.8 Hz, 8-H), 7.60(1H, dd, J = 6.4, 1.1 Hz, 6′-H), 7.40(1H, dd, J = 7.6, 1.1 Hz, 7-H), 7.27(1H, td, J = 5.6, 1.0 Hz, 4′-H), 7.05(1H, d, J = 7.2 Hz, 3′-H), 6.91(1H, td, J = 7.2, 1.1 Hz, 5′-H); ^{13}C NMR ($CDCl_3$, 100 MHz) δ 157.3, 147.2, 143.3, 130.4, 126.0, 124.3, 124.3, 121.2, 121.1, 119.2, 117.9, 117.4, 115.4, 107.9; HRMS (FAB/Double-focusing magnetic sector), m/z Calcd. For $C_{14}H_{10}F_3N_2O$ 279.0745, found 279.0737.

*6-Cyano HPIP (**11**).* Purification by a silica gel column chromatography ($CHCl_3$) and recrystallized from ethanol afforded **11** as white solid (419 mg, 44%): mp 246.2−247.2 °C; ^{1}H NMR ($CDCl_3$, 400 MHz) δ 12.06 (1H, s, OH), 8.61(1H, s, 5-H), 7.97(1H, s, 3-H), 7.70(1H, d, J = 6.0 Hz, 8-H), 7.60(1H, dd, J = 5.3, 1.0 Hz, 6′-H), 7.37(1H, dd, J = 5.8, 1.0 Hz, 7-H), 7.30(1H, td, J = 7.0, 1.0 Hz, 4′-H), 7.05(1H, d, J = 5.3 Hz, 3′-H), 6.92(1H, td, J = 6.8, 1.0 Hz, 5′-H); ^{13}C NMR ($CDCl_3$, 100 MHz) δ 157.4, 147.8, 142.9, 131.0, 130.8, 126.1, 125.2, 119.4, 118.1, 117.7, 116.2, 115.0, 107.6, 99.6. Anal. Calcd for $C_{14}H_9N_3O$: C,71.48; H,3.86; N,17.86%. Found: C,71.79; H,3.83; N,18.04%.

*4′-Methoxy HPIP (**12**).* A chloroform (50 mL) solution of 2-acetyl-5-methoxyphenol (1.22 g, 7.34 mmol) and copper(II) bromide (2.95 g, 13.2 mmol) was refluxed for 24 h. After cooling, filtering off insoluble solid, evaporation of the filtrate yielded crude 2-(bromoacetyl)-5-methoxyphenol, which was applied to a silica gel column (ethyl acetate/hexane = 1:5; 50%). Then an acetonitrile (40 mL) solution of 2-(bromoacetyl)-5-methoxyphenol (869 mg, 3.55 mmol), 2-aminopyridine (334 mg, 3.55 mmol) and $NaHCO_3$ (596 mg, 7.10 mmol) was refluxed for 20 h. After filtering off insoluble solid and evaporation, the crude product was purified by a silica gel column chromatography (ethyl acetate/hexane = 1:1). Recrystallization from ethanol gave **12** as a white crystal (342 mg, 40%): mp 158.0−158.3 °C; ^{1}H NMR ($CDCl_3$, 400 MHz) δ 12.87 (1H, s, OH), 8.14 (1H, dt, J = 6.7, 1.1 Hz, 5-H), 7.76 (1H, s, 3-H), 7.57 (1H, dd, J = 9.2, 0.9 Hz, 8-H), 7.49 (1H, d, J = 8.2 Hz, 6′-H), 7.21 (1H, ddd, J = 8.9, 6.9, 1.1 Hz, 7-H), 6.84 (1H, td, J = 6.9, 1.4 Hz, 6-H), 6.59 (1H, d, J = 2.7 Hz, 3′-H), 6.48 (1H, dd, J = 8.7, 2.7 Hz5′-H), 3.83 (3H, s, OCH_3); ^{13}C NMR ($CDCl_3$, 100 MHz) δ 161.0, 158.9, 145.4, 143.3, 126.6, 125.2, 124.9, 116.5, 112.9, 109.3, 106.5, 105.5, 101.7, 55.3. Anal. Calcd for $C_{14}H_{12}N_2O_2$: C,69.99; H,5.03; N,11.66%. Found: C,70.17; H,5.03; N,11.50%.

*5′-Methyl-6-chloro HPIP (**13**).* A chloroform (50 mL) solution of 2-acetyl-4-methylphenol (3.00 g, 20.0 mmol) and copper(II) bromide (6.70 g, 30.0 mmol) was refluxed for 22 h. After cooling, filtering off insoluble solid, evaporation of the filtrate yielded crude 2-(bromoacetyl)-4-methylphenol, which was applied to a silica gel column ($CHCl_3$/hexane = 1:1; 66%). Then an acetonitrile (30 mL)

dx.doi.org/10.1021/jo302711t | J. Org. Chem. XXXX, XXX, XXX−XXX

solution of 2-(bromoacetyl)-4-methylphenol (417 mg, 1.82 mmol), 2-amino-5-chloropyridine (234 mg, 1.82 mmol) and $NaHCO_3$ (306 mg, 3.64 mmol) was refluxed for 26 h. After cooling, insoluble solid was filtered off. Evaporation of the filtrate afforded crude product, which was then purified by a silica gel column chromatography ($CHCl_3$). Recrystallization from ethanol gave **13** as a white crystal (246 mg, 52%): mp 199.6−200.4 °C; ^{1}H NMR ($CDCl_3$, 400 MHz) δ 12.18 (1H, s, OH), 8.20 (1H, d, J = 1.1 Hz, 5-H), 7.84 (1H, s, 3-H), 7.54 (1H, d, J = 9.9 Hz, 8-H), 7.37 (1H, d, J = 1.6 Hz, 6′-H), 7.20 (1H, dd, J = 9.3, 2.2 Hz, 7-H), 7.06 (1H, dd, J = 8.2, 2.2 Hz, 4′-H), 6.94 (1H, d, J = 8.2 Hz, 3′-H), 2.32 (3H, s, CH_3); ^{13}C NMR ($CDCl_3$, 100 MHz) δ 155.0, 146.4, 141.8, 130.8, 128.1, 126.4, 125.9, 123.1, 121.2, 117.5, 117.0, 115.2, 107.0, 20.6. Anal. Calcd for $C_{14}H_{11}ClN_2O$: C,65.00; H,4.29; N,10.83%. Found: C,64.89; H,4.27; N,10.65%.

5′-Methyl-6-trifluoromethyl HPIP (14). A chloroform (50 mL) solution of 2-acetyl-4-methylphenol (3.00 g, 20.0 mmol) and copper(II) bromide (6.70 g, 30.0 mmol) was refluxed for 22 h. After cooling, filtering off insoluble solid, evaporation of the filtrate yielded crude 2-(bromoacetyl)-4-methylphenol, which was applied to a silica gel column ($CHCl_3$/hexane = 1:1; 66%). Then an acetonitrile (30 mL) solution of 2-(bromoacetyl)-4-methylphenol (1.29 g, 5.63 mmol), 2-amino-5-chloropyridine (915 mg, 5.64 mmol) and $NaHCO_3$ (576 mg, 6.85 mmol) was refluxed for 15 h. After cooling, insoluble solid was filtered off. Evaporation of the filtrate afforded crude product, which was then purified by a silica gel column chromatography ($CHCl_3$). Recrystallization from ethanol gave **14** as a white crystal (1.12 g, 68%): mp 181.2−182.2 °C; ^{1}H NMR ($CDCl_3$, 400 MHz) δ 12.04 (1H, s, OH), 8.53 (1H, s, 5-H), 7.96 (1H, s, 3-H), 7.70 (1H, d, J = 9.6 Hz, 8-H), 7.38−7.52 (2H, m, 6′,7-H), 7.08 (1H, d, J = 8.4 Hz, 4′-H), 6.96 (1H, d, J = 8.4 Hz, 3′-H), 2.33 (3H, s, CH_3); ^{13}C NMR ($CDCl_3$, 100 MHz) δ 155.0, 147.2, 143.2, 131.2, 128.2, 126.1, 124.7, 124.2, 124.2, 122.0, 121.0, 117.6, 117.2, 114.9, 107.8, 20.5. Anal. Calcd for $C_{15}H_{11}F_3N_2O$: C,61.64; H,3.79; N,9.59%. Found: C,61.47; H,3.76; N,9.42%.

■ ASSOCIATED CONTENT

Ⓢ Supporting Information

^{1}H and ^{13}C NMR spectra of **2**−**14** (Figures S1−S26), the calculated energy levels of $HOMO_{IPT}$ and $LUMO_{IPT}$, and the lowest transition energy (ΔE) obtained using the CIS-method in the intramolecular hydrogen-transferred (IPT) state of **1**−**14** (Table S1). This material is available free of charge via the Internet at http://pubs.acs.org.

■ AUTHOR INFORMATION

Corresponding Author

*E-mail: araki@iis.u-tokyo.ac.jp, mutai@iis.u-tokyo.ac.jp.

Notes

The authors declare no competing financial interest.

■ ACKNOWLEDGMENTS

This work was supported by Grants-in-Aid for Scientific Research (B) (No. 21350109) and (C) (No. 24550222) from the Japan Society for the Promotion of Science (JSPS), and Promotion of Scientific Research (0241027-A) from the Iketani Science and Technology Foundation, Japan.

■ REFERENCES

(1) (a) Sasabe, H.; Kido, J. *Chem. Mater.* **2011**, *23*, 621−630. (b) Zhao, Y. S.; Fu, H.; Peng, A.; Ma, Y.; Liao, Q.; Yao, J. *Acc. Chem. Res.* **2010**, *43*, 409−418. (c) Qian, G.; Wang, Z. Y. *Chem.—Asian J.* **2010**, *5*, 1006−1029. (d) Kamtekar, K. T.; Monkman, A. P.; Bryce, M. R. *Adv. Mater.* **2010**, *22*, 572−582. (e) Ooyama, Y.; Harima, Y. *Eur. J. Org. Chem.* **2009**, 2903−2934. (f) Samuel, I. D. W.; Turnbull, G. A. *Chem. Rev.* **2007**, *107*, 1272−1295. (g) Barbarella, G.; Melucci, M.; Sotgiu, G. *Adv. Mater.* **2005**, *17*, 1581−1593. (h) Coe, S.; Woo, W.-K.; Bawendi, M.; Bulovíc, V. *Nature* **2002**, *420*, 800−803. (i) Irie, M.; Fukaminato, T.; Sasaki, T.; Tamai, N.; Kawai, T. *Nature* **2002**, *420*, 759−760. (j) Taniguchi, Y. *J. Photopolym. Sci. Technol.* **2002**, *15*, 183−184. (k) Mitschke, U.; Bauerle, P. *J. Mater. Chem.* **2000**, *10*, 1471−1507.

(2) (a) Review of the aggregation-induced emission enhancement (AIEE): Hong, Y.; Lama, J. W. Y.; Tang, B.-Z. *Chem. Soc. Rev.* **2011**, *40*, 5361−5388. (b) Mutai, T.; Satou, H.; Araki, K. *Nat. Mater.* **2005**, *4*, 685−687. (c) An, B.-K.; Kwon, S.-K.; Jung, S.-D.; Park, S.-Y. *J. Am. Chem. Soc.* **2002**, *124*, 14410−14415. (d) Hirano, K.; Minakata, S.; Komatsu, M. *J. Phys. Chem. A* **2002**, *106*, 4868−4871. (e) Luo, J.; Xie, Z.; Lam, J. W. Y.; Cheng, L.; Chen, H.; Qiu, C.; Kwok, H.-S.; Zhan, X.; Liu, Y.; Zhu, D.; Tang, B.-Z. *Chem. Commun.* **2001**, 1740−1741.

(3) Douhal, A.; Lahmani, F.; Zewail, A. H. *Chem. Phys.* **1996**, *207*, 477−498.

(4) (a) Barbatti, M.; Aquino, A. J. A.; Lischka, H.; Schriever, C.; Lochbrunner, S.; Riedle, E. *Phys. Chem. Chem. Phys.* **2009**, *11*, 1406−1415. (b) Lochbrunner, S.; Schultz, T.; Schmitt, M.; Shaffer, J. P.; Zgierski, M. Z.; Stolow, A. *J. Chem. Phys.* **2001**, *114*, 2519−2522.

(5) Ormson, S. M.; Brown, R. G. *Prog. React. Kinet.* **1994**, *19*, 45−91.

(6) (a) Konoshima, H.; Nagao, S.; Kiyota, I.; Amimoto, K.; Yamamoto, N.; Sekine, M.; Nakata, M.; Furukawa, K.; Sekiya, H. *Phys. Chem. Chem. Phys.* **2012**, *14*, 16448−16457. (b) Furukawa, K.; Yamamoto, N.; Nakabayashi, T.; Ohta, N.; Amimoto, K.; Sekiya, H. *Chem. Phys. Lett.* **2012**, *539*−*540*, 45−49. (c) Tsai, H.-H.; G.; Sun, H.-L. S.; Tan, C.-J. *J. Phys. Chem. A* **2010**, *114*, 4065−4079. (d) Henary, M. M.; Wu, Y.; Cody, J.; Sumalekshmy, S.; Li, J.; Mandal, S.; Fahrni, C. J. *J. Org. Chem.* **2007**, *72*, 4784−4797. (e) Ouyang, J.; Ouyang, C.; Fujii, Y.; Nakano, Y.; Shoda, T.; Nagano, T. *J. Heterocycl. Chem.* **2004**, *41*, 359−365. (f) Das, K.; Sarkar, N.; Majumda, D.; Bhattacharyya, K. *Chem. Phys. Lett.* **1992**, *198*, 443−448.

(7) (a) Seo, J.; Kim, S.; Park, S. Y.; Park, S. Y. *Bull. Korean Chem. Soc.* **2005**, *26*, 1706−1710. (b) Chen, W.; Twum, E. B.; Li, L.; Wright, B. D.; Rinaldi, P. L.; Pang, Y. *J. Org. Chem.* **2012**, *77*, 285−290. (c) Ohshima, A.; Momotake, A.; Nagahata, R.; Arai, T. *J. Phys. Chem. A* **2005**, *109*, 9731−9736. (d) Wang, H.; Zhang, H.; Abou-Zied, O.; K.; Yu, C.; Romesberg, F. E.; Glasbeek, M. *Chem. Phys. Lett.* **2003**, *367*, 599−608.

(8) (a) Ma, J.; Zhao, J.; Yang, P.; Huang, D.; Zhang, C.; Li, Q. *Chem. Commun.* **2012**, *48*, 9720−9722. (b) Yao, D.; Zhao, S.; Guo, J.; Zhang, Z.; Zhang, H.; Liu, Y.; Wang, Y. *J. Mater. Chem.* **2011**, *21*, 3568−3570. (c) Mohammed, O. F.; Luber, S.; Batista, V. S.; Nibbering, E. T. J. *J. Phys. Chem. A* **2011**, *115*, 7550−7558. (d) Rini, M.; Dreyer, J.; Nibbering, E. T. J.; Elsaesser, T. *Chem. Phys. Lett.* **2003**, *374*, 13−19. (e) Frey, W.; Laermer, F.; Elsaesser, T. *J. Phys. Chem.* **1991**, *95*, 10391−10395. (f) Anthony, K.; Brown, R. G.; Hepworth, J. D.; Hodgson, K. W.; May, B.; West, M. A. *J. Chem. Soc., Perkin Trans. 2* **1984**, 2111−2117.

(9) Kwon, J. E.; Park, S. Y. *Adv. Mater.* **2011**, *23*, 3615−3642.

(10) (a) Seo, J.; Kima, S.; Lee, Y.-S.; Kwon, O.-H.; Park, K. H.; Choi, S. Y.; Chung, Y. K.; Jang, D.-J.; Park, S. Y. *J. Photochem. Photobiol., A* **2007**, *191*, 51−58. (b) Chuang, W.-T.; Hsieh, C.-C.; Lai, C.-H.; Lai, C.-H.; Shih, C.-W.; Chen, K.-Y.; Hung, W.-Y.; Hsu, Y.-H.; Chou, P.-T. *J. Org. Chem.* **2011**, *76*, 8189−8202.

(11) Mutai, T.; Tomoda, H.; Ohkawa, T.; Yabe, Y.; Araki, K. *Angew. Chem., Int. Ed.* **2008**, *47*, 9522−9524.

(12) (a) Park, S.; Seo, J.; Kim, S. H.; Park, S. Y. *Adv. Funct. Mater.* **2008**, *18*, 726−731. (b) Hu, Y.; Zhang, Y.; Liang, F.; Wang, L.; Ma, D.; Jing, X. *Synth. Met.* **2003**, *137*, 1123−1124.

(13) (a) Park, S.; Kwon, J. E.; Kim, S. H.; Seo, J.; Chung, K.; Park, S.-Y.; Jang, D.-J.; Medina, B. M.; Gierschner, J.; Park, S. Y. *J. Am. Chem. Soc.* **2009**, *131*, 14043−14049. (b) Kim, S.; Seo, J.; Jung, H. K.; Kim, J. -J.; Park, S.-Y. *Adv. Mater.* **2005**, *17*, 2077−2082. (c) Chang, S. M.; Tzeng, Y. J.; Wu, S. Y.; Li, K. Y.; Hsueh, K. L. *Thin Solid Films* **2005**, *477*, 38−41.

(14) (a) Shono, H.; Ohkawa, T.; Tomoda, H.; Mutai, T.; Araki, K. *ACS Appl. Mater. Interfaces* **2011**, *3*, 654−657. (b) Tang, K.-C.; Chang, M.-J.; Lin, T.-Y.; Pan, H.-A.; Fang, T.-C.; Chen, K.-Y.; Hung, W.-Y.; Hsu, Y.-H.; Chou, P.-T. *J. Am. Chem. Soc.* **2011**, *133*, 17738−17745.

(c) Sun, W.; Li, S.; Hu, R.; Qian, Y.; Wang, S.; Yang, G. *J. Phys. Chem. A* **2009**, *113*, 5888−5895. (d) Chen, K.-Y.; Hsieh, C.-C.; Cheng, Y.-M.; Lai, C.-H.; Chou, P.-T. *Chem. Commun.* **2006**, 4395−4397.
(15) Douhal, A.; Amat-Guerri, F.; Acuña, A. U. *J. Phys. Chem.* **1995**, *99*, 76−80.
(16) Douhal, A. *Ber. Bunsen-Ges.* **1998**, *102*, 448−451.
(17) (a) Douhal, A.; Amat-Guerri, F.; Acuña, A. U. *Angew. Chem., Int. Ed. Engl.* **1997**, *36*, 1514−1516. (b) Stasyuk, A. J.; Banasiewicz, M.; Cyrański, M. K.; Gryko, D. T. *J. Org. Chem.* **2012**, *77*, 5552−5558.
(18) Shigemitsu, Y.; Mutai, T.; Houjou, H.; Araki, K. *J. Phys. Chem. A* **2012**, *116*, 12041−12048.
(19) Grabowski, Z. R.; Rotkiewicz, K.; Rettig, W. *Chem. Rev.* **2003**, *103*, 3899−4031.
(20) Yang, X.; Lu, R.; Zhou, H.; Xue, P.; Wang, F.; Chen, P.; Zhao, Y. *J. Colloid Interface Sci.* **2009**, *339*, 527−532.
(21) (a) Namba, K.; Osawa, A.; Ishizaka, S.; Kitamura, N.; Tanino, K. *J. Am. Chem. Soc.* **2011**, *133*, 11466−11469. (b) Yamaguchi, E.; Shibahara, F.; Murai, T. *J. Org. Chem.* **2011**, *76*, 6146−6158. (c) Yamaguchi, Y.; Tanaka, T.; Kobayashi, S.; Wakamiya, T.; Matsubara, Y.; Yoshida, Z. *J. Am. Chem. Soc.* **2005**, *127*, 9332−9333.
(22) De Mello, J. C.; Wittmann, H. F.; Friend, R. H. *Adv. Mater.* **1997**, *9*, 230−232.
(23) Frisch, M. J.; Trucks, G. W.; Schlegel, H. B.; Scuseria, G. E.; Robb, M. A.; Cheeseman, J. R.; Montgomery, Jr., J. A.; Vreven, T.; Kudin, K. N.; Burant, J. C.; Millam, J. M.; Iyengar, S. S.; Tomasi, J.; Barone, V.; Mennucci, B.; Cossi, M.; Scalmani, G.; Rega, N.; Petersson, G. A.; Nakatsuji, H.; Hada, M.; Ehara, M.; Toyota, K.; Fukuda, R.; Hasegawa, J.; Ishida, M.; Nakajima, T.; Honda, Y.; Kitao, O.; Nakai, H.; Klene, M.; Li, X.; Knox, J. E.; Hratchian, H. P.; Cross, J. B.; Bakken, V.; Adamo, C.; Jaramillo, J.; Gomperts, R.; Stratmann, R. E.; Yazyev, O.; Austin, A. J.; Cammi, R.; Pomelli, C.; Ochterski, J. W.; Ayala, P. Y.; Morokuma, K.; Voth, G. A.; Salvador, P.; Dannenberg, J. J.; Zakrzewski, V. G.; Dapprich, S.; Daniels, A. D.; Strain, M. C.; Farkas, O.; Malick, D. K.; Rabuck, A. D.; Raghavachari, K.; Foresman, J. B.; Ortiz, J. V.; Cui, Q.; Baboul, A. G.; Clifford, S.; Cioslowski, J.; Stefanov, B. B.; Liu, G.; Liashenko, A.; Piskorz, P.; Komaromi, I.; Martin, R. L.; Fox, D. J.; Keith, T.; Al-Laham, M. A.; Peng, C. Y.; Nanayakkara, A.; Challacombe, M.; Gill, P. M. W.; Johnson, B.; Chen, W.; Wong, M. W.; Gonzalez, C.; Pople, J. A. *Gaussian 03*, Revision C.02; Gaussian, Inc.: Wallingford, CT, 2004.